JACS
JOURNAL OF THE AMERICAN CHEMICAL SOCIETY

Article

pubs.acs.org/JACS

Photochemistry of 2-Formylphenylnitrene: A Doorway to Heavy-Atom Tunneling of a Benzazirine to a Cyclic Ketenimine

Cláudio M. Nunes,*[,†] Igor Reva,[†] Sebastian Kozuch,[‡] Robert J. McMahon,[§] and Rui Fausto[†]

[†]CQC, Department of Chemistry, University of Coimbra, 3004-535 Coimbra, Portugal
[‡]Department of Chemistry, Ben-Gurion University of the Negev, Beer-Sheva 841051, Israel
[§]Department of Chemistry, University of Wisconsin-Madison, Madison, Wisconsin 53706-1322, United States

Supporting Information

ABSTRACT: The slippery potential energy surface of aryl nitrenes has revealed unexpected and fascinating reactions. To explore such a challenging surface, one powerful approach is to use a combination of a cryogenic matrix environment and a tunable narrowband radiation source. In this way, we discovered the heavy-atom tunneling reaction involving spontaneous ring expansion of a fused-ring benzazirine into a seven-membered ring cyclic ketenimine. The benzazirine was generated in situ by the photochemistry of protium and deuterated triplet 2-formylphenylnitrene isolated in an argon matrix. The ring-expansion reaction takes place at 10 K with a rate constant of $\sim 7.4 \times 10^{-7}$ s^{-1}, despite an estimated activation barrier of 7.5 kcal mol^{-1}. Moreover, it shows only a marginal increase in the rate upon increase of the absolute temperature by a factor of 2. Computed rate constants with and without tunneling confirm that the reaction can only occur by a tunneling process from the ground state at cryogenic conditions. It was also found that the ring-expansion reaction rate is more than 1 order of magnitude faster when the sample is exposed to broadband IR radiation.

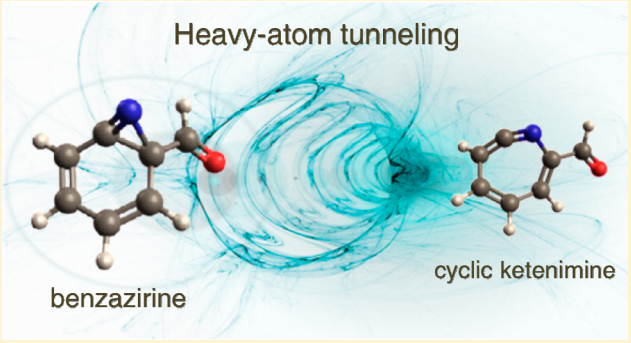

INTRODUCTION

Aryl nitrenes (Ar−N) are highly reactive intermediates most commonly generated from aryl azides (Ar−N_3).[1−3] To shed light on the aryl azides/nitrenes chemistry and on the nature of aryl nitrene species, many studies have been carried out in last 50 years, in particular, with the application of matrix isolation, time-resolved spectroscopy, and quantum-mechanical computational approaches.[1−7] This knowledge has played a crucial role for the design of aryl azides that render aryl nitrenes with suitable reactivity for uses in photoresists, in photoaffinity labeling of biomolecules, and in the design of materials or organic molecules.[8−11]

It is now well established that the photolysis of aryl azides occurs with the release of molecular nitrogen and the formation of open-shell singlet (OSS) aryl nitrene intermediates (Scheme 1). The OSS aryl nitrenes are ∼15 kcal mol^{-1} more energetic than their triplet ground state.[6,12,13] Therefore, upon formation of OSS aryl nitrenes, either relaxation by intersystem crossing (ISC) to triplet aryl nitrenes or competitive rearrange to benzazirines takes place, or both, depending on the experimental conditions and on the characteristics of the aryl substituents. With a few exceptions, the formation of benzazirines is the rate-limiting step of the process of aryl nitrene isomerization to cyclic ketenimines. The barrier of ring expansion from benzazirines to cyclic ketenimines is quite small (∼3 kcal mol^{-1} computed for parent species),[6,14] which makes very challenging and rare the capture and direct observation of benzazirines.[15−18]

Scheme 1. General Mechanism for the Photochemistry of Aryl Azides

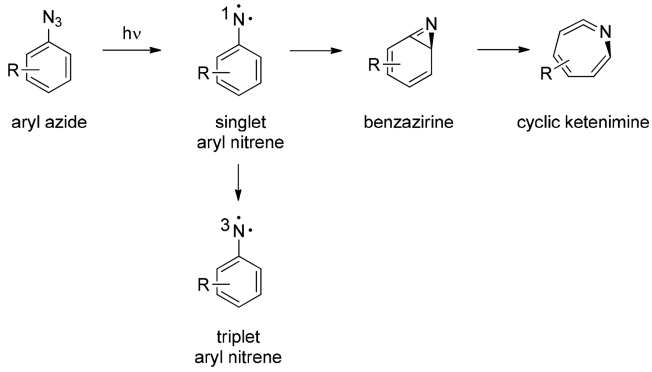

The slippery potential energy surface of aryl nitrenes hides, however, other fascinating reactions. Some of us have recently found the first indication of heavy-atom tunneling for the ring expansion of a benzazirine to a cyclic ketenimine.[15] It was observed that methylthio-substituted benzazirine, generated in the photochemistry of 4-methylthiophenylazide, spontaneously

Received: October 2, 2017
Published: November 7, 2017

DOI: 10.1021/jacs.7b10495
J. Am. Chem. Soc. 2017, 139, 17649−17659

rearranges in cryogenic matrices to the corresponding cyclic ketenimine. In contrast, under similar conditions, methoxy-substituted benzazirine, generated in the photochemistry of 4-methoxyphenylazide, was found to be stable. Furthermore, we have also recently revealed the first direct evidence of a tunneling reaction in aryl nitrene chemistry.[19] It was found that triplet 2-formylphenylnitrene ^{3}**2**-h, generated from 2-formylphenylazide **1**-h, spontaneously rearranges into iminoketene **3**-h in the dark at 10 K (Scheme 2). Under the same conditions,

Scheme 2. Tunneling Reaction of Triplet 2-Formylphenylnitrene ^{3}2-h to Iminoketene 3-h Directly Observed in Noble Gas (Ng) Cryogenic Matrices[19]

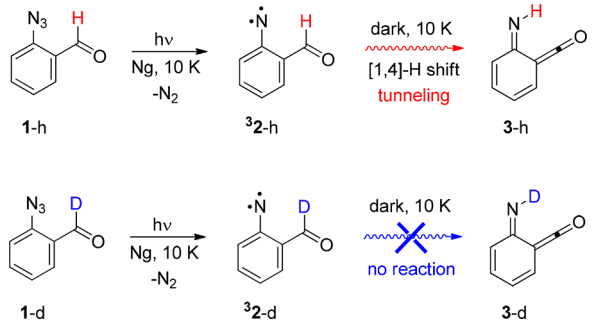

the deuterium derivative ^{3}**2**-d was observed to be stable, strongly supporting the occurrence of a tunneling mechanism as opposed to a thermally activated process.

Quantum-mechanical tunneling is an intriguing phenomenon that is becoming recognized as crucial to understand the reactivity of some organic reactions and even some biological processes that involve displacement of a light hydrogen atom.[20−23] Because the quantum-tunneling probability decreases exponentially with the square root of the shifting mass, the observation of heavy-atom tunneling (involving the displacement of non-hydrogen atoms) is rare.[24] There are six reactions known where experimental evidence was obtained for heavy-atom tunneling occurring under cryogenic conditions from the ground vibrational state:[25] the automerization of cyclobutadiene,[26] the ring-expansion reactions of methylcyclobutylfluorocarbene,[27] noradamantylchlorocarbene,[28] strained cyclopropane 1*H*-bicyclo[3.1.0]-hexa-3,5-dien-2-one,[29] and methylthio-substituted benzazirine,[15] and the Cope rearrangement of dimethylsemibullvalene.[30] Nonetheless, computational chemists have been discovering and predicting that carbon atom tunneling would contribute to many more reactions.[24,31]

Herein, we report new results obtained in the quest for elusive reactions on potential energy surface of aryl nitrenes. Using low-temperature matrix isolation coupled with IR spectroscopy and a tunable narrowband radiation source, the photochemistry of protium ^{3}**2**-h and deuterated ^{3}**2**-d triplet 2-formylphenylnitrene was investigated and one interesting case of heavy-atom tunneling consisting in the ring-expansion reaction of the corresponding benzazirine to cyclic ketenimine was discovered. Computations performed using small curvature tunneling approximation and canonical variational transition-state theory confirm that the reaction can only occur by a tunneling process from the ground state at cryogenic conditions.

RESULTS AND DISCUSSION

Photochemistry of 2-Formylphenylnitrene. Few minutes irradiation at λ = 308 nm of deuterated 2-formylphenylazide **1**-d, isolated in an argon matrix at 10 K, gives mainly triplet deuterated 2-formylphenylnitrene ^{3}**2**-d.[32] As shown in Figure 1, the experimental IR bands of the photoproduct are in

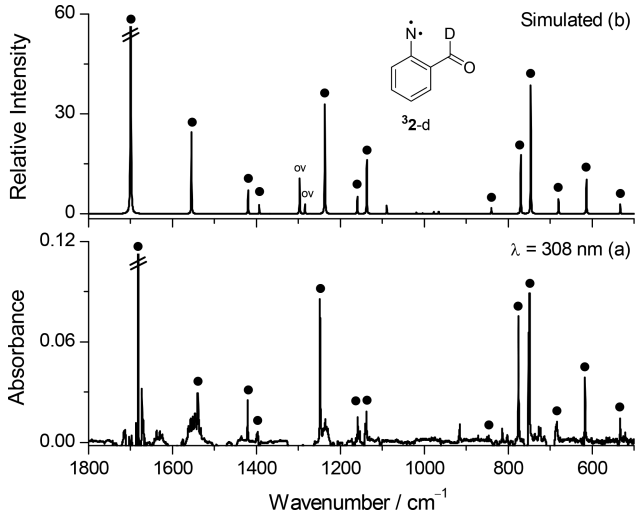

Figure 1. (a) Experimental difference IR spectrum obtained as the spectrum after UV irradiation at λ = 308 nm (240 s, 3 mW) of deuterated 2-formylphenylazide **1**-d isolated in an argon matrix at 10 K "minus" the spectrum of **1**-d before irradiation. The negative bands (truncated) are due to the consumed **1**-d (at this stage ∼60%). The positive bands labeled with black circles (●) are assigned to triplet deuterated 2-formylphenylnitrene ^{3}**2**-d. (b) IR spectrum of ^{3}**2**-d simulated at the B3LYP/6-311++G(d,p) level. The labels "ov" indicate IR bands of ^{3}**2**-d overlapped with more intense bands due to the **1**-d precursor.

excellent agreement with the IR spectrum of ^{3}**2**-d calculated at the B3LYP/6-311++G(d,p) level. The comprehensive assignment of the experimental IR spectrum of triplet deuterated 2-formylphenylnitrene ^{3}**2**-d is given in Table S1. The irradiation, under similar conditions, of protium 2-formylphenylazide **1**-h produces mainly triplet 2-formylphenylnitrene ^{3}**2**-h, which spontaneously rearranges by tunneling to iminoketene **3**-h.[19] In contrast to the behavior of nitrene ^{3}**2**-h, deuterated nitrene ^{3}**2**-d is stable against tunneling in argon matrix at 10 K.

Subsequently, the photochemistry of ^{3}**2**-d was investigated by performing irradiations using longer wavelengths, where the remaining precursor **1**-d does not absorb. Starting with irradiations at λ = 600 nm and gradually decreasing the wavelength, it was found that nitrene ^{3}**2**-d starts to react at around λ = 530 nm.[33] Figure 2 shows the results of irradiation at λ = 530 nm during a total time of 40 min, when the consumption of ^{3}**2**-d is ∼70%. Concomitantly with consumption of ^{3}**2**-d, at least three different photoproducts labeled as **A** (2112 cm^{-1}), **B** (1839 cm^{-1}) and **C** (1695/1688 cm^{-1}) were identified. The amount of photoproduct **A** was found to reach its maximum at the current stage of irradiation (t = 40 min). The continuation of irradiation (λ = 530 nm) led to a decrease in the total amount of **A** and a significant increase in the total amount of **B** (Figure S1). This kinetic trend strongly suggests that **B** is not directly formed from the nitrene ^{3}**2**-d.

DOI: 10.1021/jacs.7b10495
J. Am. Chem. Soc. 2017, 139, 17649−17659

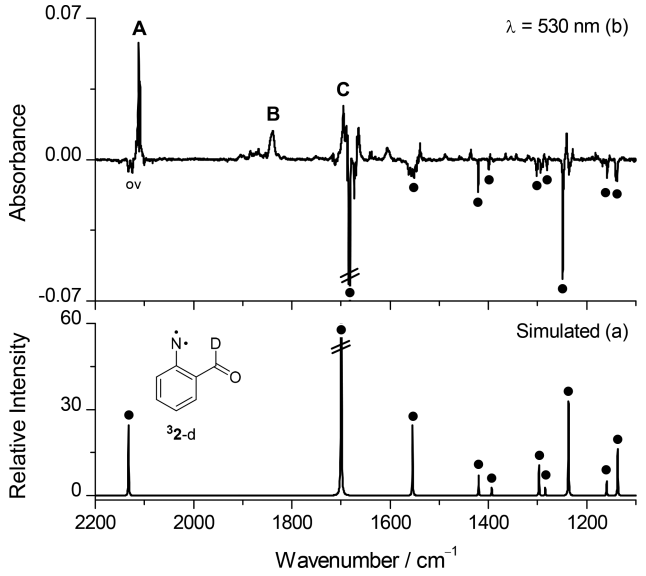

Figure 2. (a) IR spectrum of triplet deuterated 2-formylphenylnitrene ^{3}**2**-d simulated at the B3LYP/6-311++G(d,p) level. (b) Experimental difference IR spectrum showing changes after irradiation at λ = 530 nm (40 min, 90 mW), subsequent to irradiation at λ = 308 nm (see Figure 1). The negative bands are due to the consumed nitrene ^{3}**2**-d (at this stage ~70%). The positive bands labeled **A**−**C** are the most characteristic bands of the identified photoproducts. The label "ov" indicates an IR band of ^{3}**2**-d overlapped with a more intense band due to the photoproduct **A**.

Indeed, after the irradiation at λ = 530 nm during a total time of 160 min (when almost all nitrene ^{3}**2**-d is consumed; Figure S1), it was found that subsequent irradiation at λ = 500 nm converts **A** into **B** (Figure 3b).[34] The experimental IR signature of the consumed **A** compares very well with the IR spectrum of N-deuterated iminoketene **3**-d calculated at the B3LYP/6-311++G(d,p) level (Figure 3a,b). The most intense band observed in the IR spectrum of **A** appears at 2112 cm^{-1}, a frequency region where ketenes usually have characteristic strong ν(C═C═O)$_{as}$ absorption (e.g., typically around 2100 cm^{-1}).[35] Actually, this band compares well with the ν(C═C═O)$_{as}$ band described at 2110 cm^{-1} for the protium iminoketene **3**-h analogue, which is formed by 2-formylphenylnitrene ^{3}**2**-h tunneling.[19] Other characteristic IR bands of **A** are observed at 1637, 1547, 1540, and 621/616 cm^{-1}, in good correspondence with the IR bands of **3**-d calculated at 1645 [ν(C═C)$_{as}$], 1555 [ν(C═N)], 1541 [ν(C═C)$_s$], and 607 [τ(N−D)] cm^{-1}. A more comprehensive assignment of the observed IR spectrum of product **A**, identified as N-deuterated iminoketene **3**-d, is given in Table S2.

The experimental IR signature of the photoproduct **B** was found to compare very well with the IR spectrum of N-deuterated benzoazetinone **4**-d calculated at the B3LYP/6-311++G(d,p) level (Figure 3b,c). The most intense band observed in the IR spectrum of **B** at 1836 cm^{-1} correlates well with the most intense band predicted in the IR spectrum of **4**-d at 1852 [ν(C═O)] cm^{-1}. This assignment is also supported by the frequency proximity between the band at 1836 cm^{-1} and the strong carbonyl stretching at 1843 cm^{-1} described for the *N*-methylbenzoazetinone analogue,[36] which are typical of the

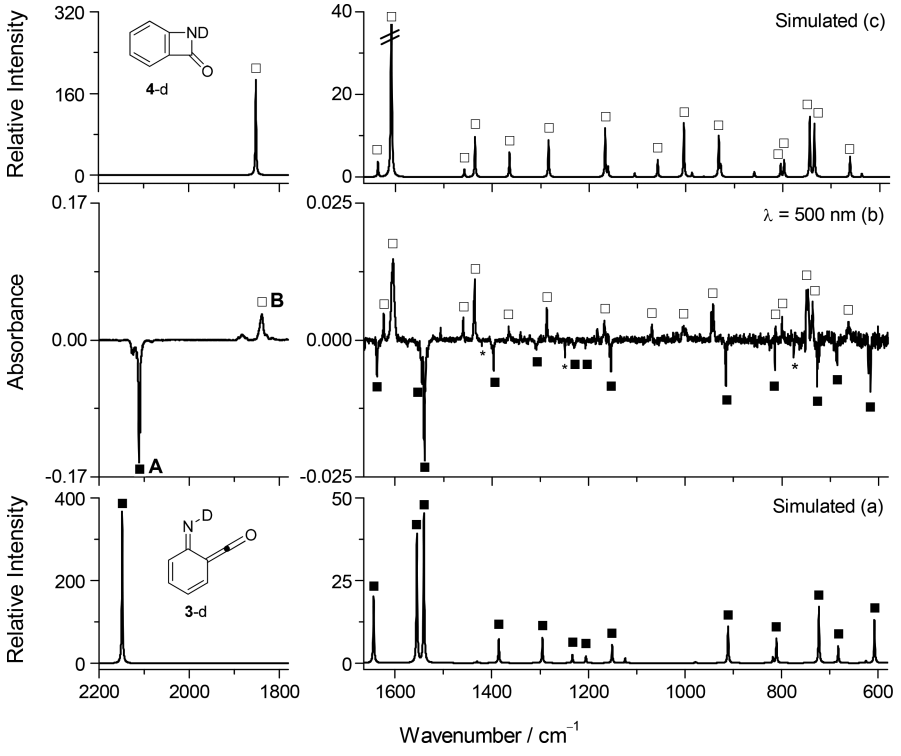

Figure 3. (a) IR spectrum of N-deuterated iminoketene **3**-d simulated at the B3LYP/6-311++G(d,p) level. (b) Experimental difference IR spectrum showing changes after irradiation at λ = 500 nm (100 min, 60 mW), subsequent to irradiation at λ = 530 nm that consumed nitrene ^{3}**2**-d (Figure S1). The negative bands are due to the consumed **A** assigned to iminoketene **3**-d (solid squares, ■). The positive bands are due to the formation of **B** assigned to benzoazetinone **4**-d (empty squares, □). Asterisks (*) indicate the bands due to traces of nitrene ^{3}**2**-d consumed. (c) IR spectrum of N-deuterated benzoazetinone **4**-d simulated at the B3LYP/6-311++G(d,p) level.

DOI: 10.1021/jacs.7b10495
J. Am. Chem. Soc. 2017, 139, 17649−17659

Table 1. Experimental IR Spectral Data (Argon Matrix at 10 K), B3LYP/6-311++G(d,p) Calculated Vibrational Frequencies (ν, cm^{-1}), Absolute Infrared Intensities (A^{th}, km mol^{-1}), and Vibrational Assignment of Deuterated Formylbenzazirine 5-d[a]

Ar matrix[b]		calculated[c]		
ν	I	ν	A^{th}	approx assignment[d,e]
2108/2097/2093	ov/br/m	2109	59.8	ν(C−D)
1751	w	1802	34.8	ν(C═N)
1706/1695/1689/1685	ov/s/s/s	1710	341.3	ν(C═O)
1595/1589	ww/vw	1586	3.7	$\nu(C{=}C)_{as}$
1488	m	1484	26.3	$\nu(C{=}C)_{s}$
1419	vw	1415	3.9	δ1(C−H)
1355	w	1351	7.0	δ2(C−H)
1241	s	1221	57.4	ν(C2−C1)
1189	vw	1183	5.5	δ3(C−H)
1143	vw	1139	6.0	δ4(C−H)
1125	br	1108	22.5	$\nu(C3{-}C2{-}C1)_{as}$, δ(C−D)
1018/1016	br	1013	23.3	δ1(6-ring)
1004	vw	997	7.8	δ(C−D)
947	vw/ov	948	5.0	γ1(C−H) + ν(C6−C5)
		936	4.4	γ1(C−H) − ν(C6−C5)
784/782	s/s	783	41.2	γ2(C−H)
747	w/ov	747	4.3	δ2(6-ring)
714/712	s/s	711	67.4	γ3(C−H)
643/640	m/w	649	8.5	τ1(6-ring)

[a]Deuterated formylbenzazirine **5**-d was generated by irradiation of deuterated 2-formylphenylnitrene ^{3}**2**-d in an argon matrix at 10 K. Only bands in the 2600−600 cm^{-1} region having calculated intensities above 3 km mol^{-1} are included. [b]Experimental intensities are presented in qualitative terms: s = strong, m = medium, w = weak, vw = very weak, br = broad, and ov = overlapped. [c]B3LYP/6-311++G(d,p) calculated scaled frequencies. [d]Assignments made by inspection of Chemcraft animations. Abbreviations: ν = stretching, δ = bending, γ = rocking, τ = torsion, s = symmetric, as = antisymmetric, and 6-ring = six-membered ring. Signs "+" and "−" designate combinations of vibrations occurring in "syn"-phase ("+") and in "anti"-phase ("−"). [e]For atom numbering see Scheme S1.

ν(C═O) frequencies where the carbonyl group is inserted in a 4-membered ring.[37] Other characteristic IR bands of **B** are observed at 2543/2533 and 1605 cm^{-1}, fitting well with the IR bands of **4**-d calculated at 2535 [ν(N−D)] and 1608 [ring stretching] cm^{-1}. A more complete assignment (total of 19 bands) of the observed IR spectrum of **B**, identified as N-deuterated benzoazetinone **4**-d, is given in Table S3.

The photochemical transformation of an iminoketene into a benzoazetinone is not unprecedented. Dunkin et al.[36] and Tomioka et al.[38] reported that analogous *N*-methyl- and *N*-methoxyiminoketenes undergo ring closure to the corresponding N-substituted benzoazetinones in an argon matrix upon irradiation with λ > 400 nm. The identification of those iminoketenes and benzoazetinones was performed mainly by their characteristic $\nu(C{=}C{=}O)_{as}$ and ν(C═O) bands, respectively (Scheme S2). In the current work, the transformation of iminoketene **3**-d into benzoazetinone **4**-d was established much more comprehensively, based on the experimental identification of the almost complete mid-IR spectra of these species.

Ring Expansion of Benzazirine into Cyclic Ketenimine. Interestingly, besides the photochemical conversion of **3**-d (**A**) into **4**-d (**B**), we found that **C** spontaneously rearranges into a new product labeled as **D** (1890/1880 cm^{-1}). To observe this transformation in detail, a new experiment was performed where first the nitrene ^{3}**2**-d was transformed by irradiation at λ = 530 nm and then the sample was kept at 10 K in the spectrometer beam for 3 days. After that time, the rearrangement of **C** into **D** was practically completed and the changes in the experimental IR spectrum were analyzed (Figure 4b). The IR spectrum of the consumed **C** is readily assigned to deuterated formylbenzazirine **5**-d based on the good agreement between the experimental and the calculated IR spectra (Figure 4a,b). The cyclization of nitrene **2**-d may proceed "toward" and "away from" the formyl substituent to give two isomeric benzazirines, each having two possible conformers regarding orientation of the formyl group (Table S4). Vibrational calculations on these four structures revealed that only **5**-d (the most stable form) is compatible with the experimental IR spectrum of **C** (Figures S2 and S3). The most characteristic IR bands of **C** are observed at ∼2100, 1751, ∼1700, and 1241 cm^{-1}, in good agreement with the estimated IR bands of **5**-d at 2109 [ν(OC−D)], 1802 [ν(C═N)], 1710 [ν(C═O)], and 1221 [ν(ODC−C)] cm^{-1}. A slight overestimation of the B3LYP calculated ν(C═N) frequency of **5**-d (∼50 cm^{-1}) is consistent with the overestimation trend observed for other benzazirines[16] (see also data presented in Table S5). A more detailed assignment of the IR spectrum of **C**, identified as benzazirine **5**-d, is given in Table 1.

The IR spectrum of the produced species **D** is assigned to deuterated formyl cyclic ketenimine **6**-d based on the good match between the experimental and calculated IR spectra (Figure 4b,c). Cyclic ketenimines are known to have a characteristic strong IR absorption near 1900 cm^{-1}, due to $\nu(C{=}C{=}N)_{as}$ vibration,[16,39−41] which correlates well with the most intense band observed in the IR spectrum of **D** at 1890/1880 cm^{-1}. Other characteristic bands of **D** are observed at 2137/2117, 1698, 1576, and ∼1525 cm^{-1} in good agreement with the estimated IR bands of **6**-d at 2128 [ν(OC−D)], 1711 [ν(C═O)], 1579 [$\nu(C{=}C)_{as}$], and 1519 [$\nu(C{=}C)_{s}$] cm^{-1}. Four different cyclic ketenimine structures may, in principle, be formed in the chemistry of nitrene **2**-d (Table S6). Based on vibrational calculations, only the **6**-d form matches the experimental IR spectrum of **D** (Figures S4 and S5). The

DOI: 10.1021/jacs.7b10495
J. Am. Chem. Soc. 2017, 139, 17649−17659

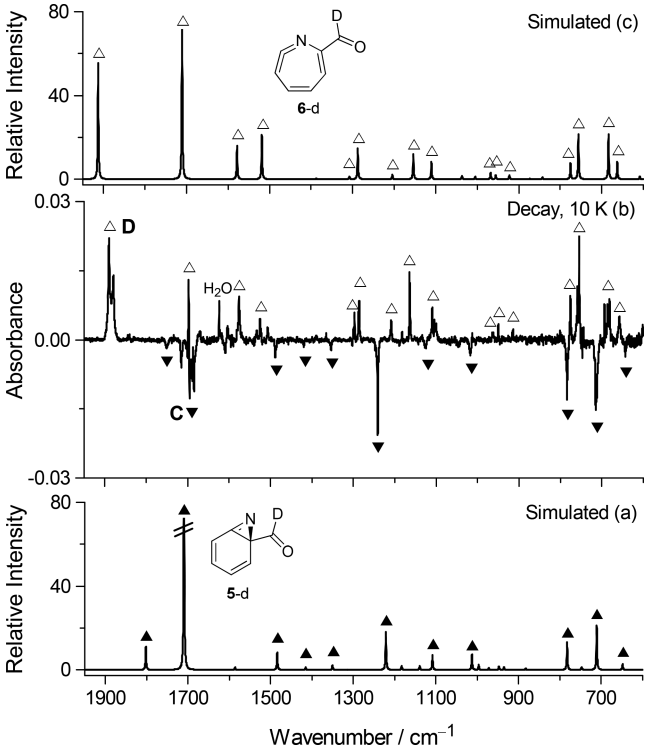

Figure 4. (a) IR spectrum of deuterated formylbenzazirine **5**-d simulated at the B3LYP/6-311++G(d,p) level. (b) Experimental difference IR spectrum showing changes occurred after keeping the sample at 10 K in the spectrometer beam for ~3 days, subsequent to irradiation at λ = 530 nm that consumed almost all triplet nitrene ^{3}**2**-d. The negative bands are due to the consumed **C** assigned to benzazirine **5**-d (solid triangles, ▲). The positive bands are due to the formation of **D** assigned to cyclic ketenimine **6**-d (empty triangles, △). (c) IR spectrum of deuterated formyl cyclic ketenimine **6**-d simulated at the B3LYP/6-311++G(d,p) level.

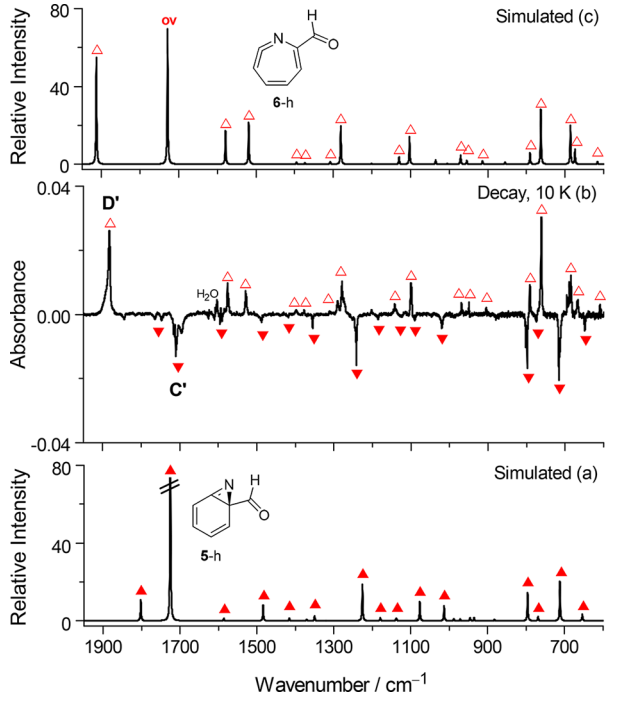

Figure 5. (a) IR spectrum of formylbenzazirine **5**-h simulated at B3LYP/6-311++G(d,p) level. (b) Experimental difference IR spectrum showing changes occurred after keeping the sample at 10 K in the spectrometer beam for 3 days, subsequent to irradiation at λ = 530 nm and after the decay of the remained triplet nitrene ^{3}**2**-h. The negative bands are due to the consumed **C′** assigned to benzazirine **5**-h (solid red triangles, ▲). The positive bands are due to the formation **D′** assigned to cyclic ketenimine **6**-h (empty red triangles, △). (c) IR spectrum of formyl cyclic ketenimine **6**-h simulated at B3LYP/6-311++G(d,p) level. The label "ov" indicates an IR band of **6**-h overlapped with a more intense band due to **5**-h

formation of this structure is in accordance with the expectations because the ring expansion via C−C cleavage in benzazirine isomer **5**-d directly results in cyclic ketenimine isomer **6**-d.[42] A detailed assignment of the IR spectrum of **D**, identified as cyclic ketenimine **6**-d, is given in Table 2.

A similar approach was applied to investigate the possibility of ring expansion in the protium benzazirine **5**-h. Triplet 2-formylphenylnitrene ^{3}**2**-h was first produced by irradiation of 2-formylphenylazide **1**-h and then immediately exposed to irradiation at λ = 530 nm. The photochemistry of ^{3}**2**-h is similar to that described for ^{3}**2**-d; at least three different products labeled as **A′** (2111 cm^{-1}), **B′** (1843 cm^{-1}), and **C′** (~1710 cm^{-1}) were formed (Figures S6 and S7). However, it must be noted that the tunneling reaction of ^{3}**2**-h to iminoketene **3**-h ($\tau_{1/2}$ ~ 6 h)[19] occurs simultaneously with the photochemistry triggered at λ = 530 nm. After 1 h of irradiation at this wavelength only a few percent of ^{3}**2**-h (<10%) remained. The nitrene ^{3}**2**-h is difficult to convert in its totality through irradiation at 530 nm on this time scale because of the formation of **3**-h (**A′**) that also absorbs at λ = 530 nm and is transformed into benzoazetinone **4**-h (**B′**). Thus, after the irradiation at λ = 530 nm, the remaining nitrene ^{3}**2**-h was first allowed to disappear in the dark by tunneling, and subsequently, the sample was kept at 10 K in the spectrometer beam for 3 days. At that time, the rearrangement of **C′** into **D′** was completed, and the IR difference spectrum corresponding to this transformation was obtained (Figure 5b).

Based on the excellent agreement between the experimental and calculated IR spectra, the consumed species **C′** was assigned to formylbenzazirine **5**-h and the produced species **D′** assigned to formyl cyclic ketenimine **6**-h (Figure 5 and Tables S7 and S8). Hence, in addition to the experiment described above for the deuterated derivative, we also found that protium benzazirine **5**-h undergoes ring expansion to cyclic ketenimine **6**-h.

Kinetics of the Benzazirine Ring Expansion to Cyclic Ketenimine. To better understand the nature of the transformation of benzazirine into cyclic ketenimine, their respective decrease and increase were followed by IR spectroscopy (using the bands at 1241 cm^{-1} for **5**-d and 1890 cm^{-1} for **6**-d for the deuterated derivative, and using the bands at 1242 cm^{-1} for **5**-h and 1883 cm^{-1} for **6**-h for the protium derivative) while keeping the sample under different given sets of conditions. For "unfiltered IR light" conditions, the kinetics of rearrangement of benzazirine **5**-d into cyclic ketenimine **6**-d was measured when the sample was kept at 10 K and permanently exposed to the IR light source of the FTIR spectrometer. As shown in Figure 6, the data are nicely fitted by equations of monoexponential decay kinetics, with a rate constant of ~1.5 × 10^{-5} s^{-1} and a half-life of ~13 h. For "dark" conditions, new experiments were performed where the sample was kept at 10 K in the dark with the only exception: when monitoring the IR spectra, we used a cutoff filter transmitting only below 2200 cm^{-1} placed between the sample and the

DOI: 10.1021/jacs.7b10495
J. Am. Chem. Soc. 2017, 139, 17649−17659

Table 2. Experimental IR Spectral Data (Argon Matrix at 10 K), B3LYP/6-311++G(d,p) Calculated Vibrational Frequencies (ν, cm^{-1}), Absolute Infrared Intensities (A^{th}, km mol^{-1}), and Vibrational Assignment of Deuterated Formyl Cyclic Ketenimine 6-d[a]

Ar matrix[b]		calculated[c]		
ν	I	ν	A^{th}	approx assignment[d,e]
2133/2117	vw/ov	2128	65.6	ν(C−D)
1890/1880	s/s	1913	175.0	ν(C═C═N)$_{as}$
1698	s/ov	1711	236.7	ν(C═O)
1576	m	1579	50.5	ν(C═C)$_{as}$
1533/1525	vw/w	1519	66.5	ν(C═C)$_{s}$
1297	w	1308	3.9	δ1(C−H)
1286	m	1288	46.3	δ2(C−H)
1208	w	1205	6.7	δ3(C−H)
1164	m	1154	38.0	ν(C2−C1)
1110/1004	w	1110	26.2	δ4(C−H)
		1037	4.9	ν(C7C6) − ν(C5C4)
		1005	3.7	δ(C−D)
965/962	vw/vw	968	9.4	ν(C7C6) + ν(C5C4)
950/949	w/w	956	5.8	γ1(C−H)
916/914	vw/vw	923	5.5	δ1(ring)
		843	3.1	γ(C−D), δ2(ring)
776	m	775	24.2	γ2(C−H)
759/756/755	m/m/s	756	68.1	γ3(C−H)
686/681	m/m	684	67.7	γ4(C−H)
658	w	663	25.9	δ(C═C═N)
602	vw	609	3.9	τ1(ring)

[a]Deuterated formyl cyclic ketenimine **6**-d was generated by ring expansion of deuterated formylbenzazirine **5**-d in an argon matrix at 10 K. Only bands in the 2600−600 cm^{-1} region having calculated intensities above 3 km mol^{-1} are included. [b]Experimental intensities are presented in qualitative terms: s = strong, m = medium, w = weak, vw = very weak, and ov = overlapped. [c]B3LYP/6-311++G(d,p) calculated scaled frequencies. [d]Assignments made by inspection of Chemcraft animations. Abbreviations: ν = stretching, δ = bending, γ = rocking, τ = torsion, s = symmetric, and as = antisymmetric. Signs "+" and "−" designate combinations of vibrations occurring in "syn"-phase ("+") and in "anti"-phase ("−"). [e]For atom numbering see Scheme S1.

spectrometer IR light source. As shown in Figure 7, under "dark" conditions (kinetics 1) only ∼25% of **5**-d rearranged to **6**-d upon 5 days. After this period of 5 days, "unfiltered IR light" conditions were applied (kinetics 2) to confirm that a much faster rate of the rearrangement occurs under the influence of IR light. The "dark" kinetics (Figure 7, kinetics 1) shows some dispersive character; i.e., it deviates from the first-order kinetics and the rate constant decreases over time. This is commonly observed for reactions in cryogenic matrices and is generally attributed to distributions of matrix sites and weak interactions between substrate and the matrix environment.[15,19,27−30] For the sake of a rough estimate, the data for "dark" kinetics were fitted by using classical equations of monoexponential decay, resulting in a rate constant of ∼7.4 × 10^{-7} s^{-1} and a half-life of ∼260 h. This "dark" rate constant is more than an order of magnitude smaller than the "unfiltered light" rate constant, unmistakably indicating a significant difference in both kinetics.

In another independent experiment, "filtered IR light" conditions were applied, whereas a cutoff filter transmitting light only below 2200 cm^{-1} was placed between the IR light source of the FTIR spectrometer and the sample. In that case,

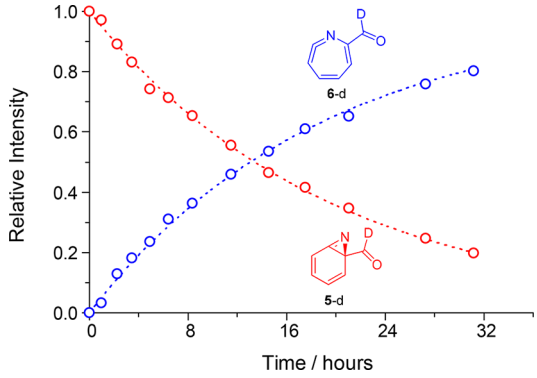

Figure 6. Kinetics of rearrangement of benzazirine **5**-d to cyclic ketenimine **6**-d in an argon matrix at 10 K, with the sample exposed to the IR light source of the FTIR spectrometer. Empty red and blue circles (○) represent the time evolution of the amounts of **5**-d (consumption, measured using the peak at 1241 cm^{-1}) and **6**-d (production, measured using the peak at 1890 cm^{-1}), respectively. Red and blue dotted lines represent best fits obtained using first-order exponential kinetics equations. The rate constants are $k_{5\text{-d}}$ = 1.4 × 10^{-5} s^{-1} and $k_{6\text{-d}}$ = 1.5 × 10^{-5} s^{-1}. More details are given in the Experimental Section.

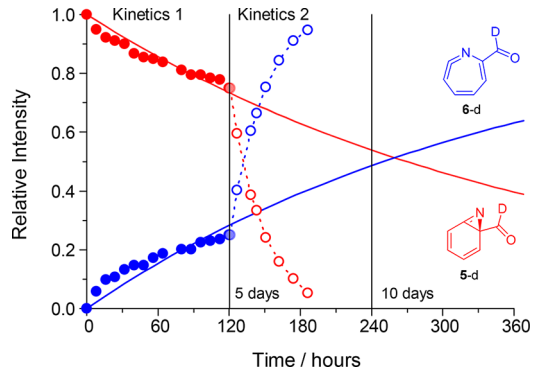

Figure 7. Kinetics of rearrangement of benzazirine **5**-d (measured using the peak at 1241 cm^{-1}) to cyclic ketenimine **6**-d (measured using the peak at 1890 cm^{-1}) in an argon matrix at 10 K. Kinetics 1 (initial 5 days, left): rearrangement of **5**-d (solid red circles (●), consumption) into **6**-d (solid blue circles (●), production) with the sample kept in the dark, except when the spectra were recorded, the sample was then protected by an infrared long-pass cutoff filter transmitting only below 2200 cm^{-1}. Kinetics 2 (after 5 days in the dark, right): rearrangement of **5**-d (empty red circles (○), consumption) into **6**-d (empty blue circles (○)), production) with the sample permanently exposed to the IR light source of the FTIR spectrometer. Blue and red solid lines represent best fits obtained using first-order single exponential kinetics equations, and adjustments were made using only the amounts of the reactant **5**-d and the product **6**-d during the first 5 days of observation (sample in the dark), corresponding to ∼25% of the conversion. The rate constants are $k_{5\text{-d}}$ = 7.1 × 10^{-7} s^{-1} and $k_{6\text{-d}}$ = 7.7 × 10^{-7} s^{-1}. Blue and red dotted lines (right) are presented to guide the eye only.

the sample was exposed to filtered light continuously (i.e., including periods between the registrations of spectra). The obtained kinetics for "filtered light" decay was found to be similar to the "dark" decay kinetics.

Experiments were also carried out to measure the kinetics of rearrangement of protium benzazirine **5**-h into protium cyclic ketenimine **6**-h. As shown in Figure S8, under "dark" conditions (kinetics 1) the rearrangement after 5 days amounts to ∼27%. Afterward, "unfiltered IR light" conditions were applied

DOI: 10.1021/jacs.7b10495
J. Am. Chem. Soc. 2017, 139, 17649−17659

(kinetics 2) and a strong increase in the reaction rate was observed, similarly to the behavior found for the deuterated derivative. Again, similarly to the deuterated compound, the kinetics of rearrangement from **5**-h to **6**-h in the dark has some dispersive character. To obtain a rough estimate, the data for "dark" kinetics were fitted by using equations of the first-order kinetics, resulting in a rate constant of ~8.8×10^{-7} s^{-1} and a half-life of ~219 h. This rate constant of the rearrangement from **5** to **6** under "dark" conditions of the protium compound differs somewhat from the analogous rate found for the deuterated analogue. Even within the measurement accuracy of peak intensities of the bands used and also with the caveat that a single-exponential fitting is only approximately applicable to trace the dispersive kinetics, these rates suggest a small decrease in the rate resulting from the substitution of protium with deuterium in the carbonyl group of **5**. Indeed, as will be shown in the next section, computations indicate that the secondary kinetic isotope effect is significant.

To verify that the rearrangement is not activated thermally, we carried out additional kinetic measurements of the rearrangement of **5**-d to **6**-d at 20 K also under "dark" conditions (Figure S9). Again, even though the kinetics has some dispersive character, the data were adjusted by using the first-order kinetic equations and a rough rate constant was estimated as ~8.9×10^{-7} s^{-1} and a half-life of ~216 h. Within the precision of estimations and considering the data from a semiqualitative perspective, the rate of the rearrangement hardly shows any increase upon increase of the absolute temperature by a factor of 2. The matrix softening induced by the temperature increase can be responsible for the possible small acceleration of the rearrangement, as proposed for other cases of tunneling reactions in matrices.[15,27−30]

CCSD(T) computations (see below) estimate an energy barrier of 7.5 kcal mol^{-1} for the rearrangement of **5** to **6** (~1.4 kcal mol^{-1} more stable). This energy barrier is far too high to afford a thermal activation at the low working temperatures up to 20 K under "dark" conditions. Moreover, attaining such a high barrier seems not possible under the experimental "filtered light" condition, when the sample at 10 K is exposed to light with wavenumbers below 2200 cm^{-1} (~6.3 kcal mol^{-1} or less). The data indicate therefore that the rearrangement of benzazirine **5** to cyclic ketenimine **6** in low temperature matrix occurs through heavy-atom tunneling. Because the reaction rate under "dark" conditions is similar to the rate when the sample is exposed to "filtered IR light" conditions, vibrationally assisted tunneling is unlikely.

In the case of "unfiltered light" conditions, the observed significantly faster rate, compared to "dark" or "filtered IR light" conditions, suggests the occurrence of IR-induced photochemistry. Here the sample is clearly exposed to light with energy well above the calculated barrier.[43] The energy deposited in vibrational modes of benzazirine **5** located above the reaction barrier, for instance into the CH stretching modes or in any overtone/combination transition with frequency above ~2625 cm^{-1} (7.5 kcal mol^{-1}), may promote isomerization to cyclic ketenimine **6** (Figure S10). In the opposite direction, from **6** to **5**, the estimated reaction barrier is higher, ca. ~8.9 kcal mol^{-1} (~3125 cm^{-1}). This barrier is above the energy of the CH stretching modes (~3000 cm^{-1}) in cyclic ketenimine **6**. Hence, the probability of depositing energy in vibrational modes above the reaction barrier is higher in **5** than in **6**, which could explain why the broadband IR irradiation tends to promote IR-induced chemistry toward **6**.[44]

Tunneling Calculations. To support the experimental evidence of a quantum tunneling effect in the process of formation of ketenimine **6** from cyclic benzazirine **5**, we computed the rate constants without and with tunneling (using canonical variational transition state theory −CVT− and small curvature tunneling −SCT−, respectively).[45] The estimated CVT rate constant at 10 K is 1.8×10^{-177} s^{-1}, which indicates that the **5**-h to **6**-h reaction is impossible to occur. In contrast, the SCT rate constant for the **5**-h to **6**-h reaction at 10 K (from the ground state at this temperature) is 3.5×10^{-5} s^{-1} (a half-life time of ~6 h), which is comparable to experimental result (around 40 times faster). The difference is justifiable considering the difference between the solid matrix experiment and the gas phase computation plus the error of the DFT theoretical method [M06-2X gives an activation energy of 6.2 kcal mol^{-1}, 1.3 kcal mol^{-1} lower than CCSD(T)]. Thus, the results validate the computational method and at the same time corroborate the observed tunneling effect of the experiments: going from **5** to **6** is a transformation only attainable by a tunneling process from the ground state at cryogenic conditions (see Figure 8). At 20 K the computed SCT rate constant is 3.6

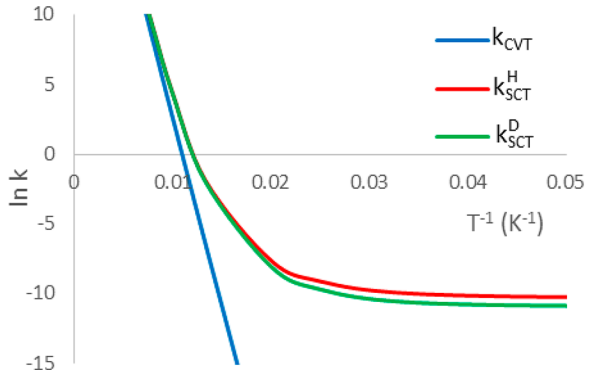

Figure 8. Arrhenius graph for the benzazirine (**5**-h and **5**-d) to cyclic ketenimine (**6**-h and **6**-d) reaction without (CVT) and with (SCT) tunneling correction. Computations indicate that below ~150 K tunneling is the main component of the rate constant and below 20 K the reaction is completely independent of the temperature (tunneling exclusively from the ground state).

$\times 10^{-5}$ s^{-1}, almost the same as at 10 K, indicating that the first vibrational excited quantum level of the reactant remains practically not thermally populated, and a thermally activated tunneling process should be negligible. This indicates that a marginal increase of the experimental rate at 20 K compared to the 10 K should be attributed to matrix softening.

We then proceeded to compute the kinetic isotope effect (KIE) not only for the formyl hydrogen but for all of the other atoms as well (using the $^{12}C/^{13}C$, $^{14}N/^{15}N$, $^{16}O/^{18}O$, and H/D mass relations). The results at 10 K are shown in Table 3. As can be seen, **5**-d indeed has a smaller rate of reaction compared to **5**-h, as was observed experimentally. The experimental KIE value was approximately 1.20 (8.8×10^{-7} s^{-1}/7.4×10^{-7} s^{-1}), while theory predicts a KIE of 1.88 (first row in Table 3); this difference can be ascribed to the same reasons explained above, but still both results clearly indicate a significant deceleration of the reaction. Notably, there is a significant negative $\Delta ZPE^{\ddagger}$ value of −0.27 kJ mol^{-1} in the H/D substitution at the formyl hydrogen which, opposite to the observed KIE, leads to an inverse semiclassical KIE and a potentially faster tunneling due to a lower barrier;[46] nevertheless, the mass effect of the

DOI: 10.1021/jacs.7b10495
J. Am. Chem. Soc. 2017, 139, 17649−17659

Table 3. Computed Kinetic Isotope Effect for the Benzazirine 5 Ring Expansion for the $^{12}C/^{13}C$, $^{14}N/^{15}N$, $^{16}O/^{18}O$, and H/D Isotopic Substitutions at 10 K

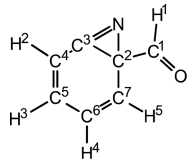

atom	KIE	atom	KIE
C^1	1.29	H^1	1.88
C^2	1.23	H^2	1.80
C^3	1.88	H^3	2.16
C^4	1.16	H^4	1.05
C^5	1.17	H^5	1.53
C^6	1.04	N	1.05
C^7	1.23	O	1.17

deuterium substitution strongly overrides this effect. Other H/D substitutions also provide a significant KIE (except for H4). In the case of heavy-atom tunneling, we can see that C3 has the largest KIE, indicating that this is the "tunneling determining atom", the one with the largest displacement. But most of other atoms also have large KIE, denoting a holistic molecular rearrangement. Interestingly the pivotal nitrogen, with a KIE of only 1.05, is comparatively static and is mostly a "spectator" in the tunneling mechanism. In this sense, the heavy atom tunneling is predominantly carbon tunneling.

CONCLUSIONS

The summary of the experimental results of the photochemistry of protium ^{3}**2**-h and deuterated ^{3}**2**-d triplet 2-formylphenylnitrene is presented in Scheme 3. Irradiation of ^{3}**2**, generated in argon matrix at 10 K from 2-formylphenylazide **1**, led to the formation of iminoketene **3** and benzazirine **5**. The iminoketene **3** was found to subsequently photorearrange to benzoazetinone **4**. The benzazirine **5** was found to undergo spontaneous ring expansion to cyclic ketenimine **6** in the dark at 10 K, despite an estimated reaction barrier of 7.5 kcal mol^{-1}. Moreover, the reaction rate was observed to barely show any increase upon increase of the absolute temperature by a factor of 2 (from 10 to 20 K). These experimental data clearly provide strong evidence that ring expansion of **5** to **6** occurs by heavy-atom tunneling. Computed rate constants with and without tunneling (SCT and CVT approximation, respectively) confirm that the ring expansion of **5** to **6** can only be attainable by a tunneling process from the ground state at cryogenic conditions. In addition, a small secondary kinetic isotopic effect, corresponding to the deceleration of the reaction upon substitution of protium with deuterium in the formyl group of benzazirine, was predicted theoretically and measured experimentally. Also interesting, it was observed that the ring expansion of **5** to **6** is stimulated by broadband IR radiation. The reaction rate was measured to be more than 1 order of magnitude faster when the sample at 10 K is exposed to the radiation from the IR light source of FTIR spectrometer.

Overall, the results unravel a remarkable feature on the potential energy surface of an aryl nitrene. We discovered two isomeric species connected photochemically that both react by quantum tunneling: the 2-formylphenylnitrene by proton tunneling, as reported previously,[19] and the corresponding benzazirine by heavy-atom tunneling, as reported here. To the best of our knowledge, this is the first system where interconverted isomers exhibit two different types of tunneling.

EXPERIMENTAL SECTION

Sample. Protium 2-formylphenylazide **1**-h and deuterated 2-formylphenylazide **1**-d were prepared as described in our previous communication.[19] The deuterium enrichment of sample **1**-d is ≥90%. Between the experiments, the samples of **1**-h or **1**-d were stored in a glass tube, under vacuum, in refrigerator at +4 °C, and in the dark. Under such conditions the azides were stable for many weeks.

Matrix Isolation IR Spectroscopy. A solid sample of **1**-h or **1**-d was placed in a glass tube that was then connected to a needle valve (SS4 BMRG valve, NUPRO) attached to the vacuum chamber of a helium-cooled cryostat (APD Cryogenics closed-cycle refrigerator with DE-202A expander). Prior to deposition of the matrices, the samples were purified from the volatile impurities by pumping through the cryostat at room temperature. The sample tube with **1**-h or **1**-d was subsequently cooled with an ice−water mixture (at 0 °C) to reduce the saturated pressure of the compound and improve the metering function of the needle valve. During the preparation of the matrices, the sample vapors were deposited, together with a large excess of argon (N60, Air Liquide) onto a CsI window at 15 K, used as optical substrate. After the deposition, all samples were cooled down to 10 K and kept at this temperature both during irradiations and during the monitoring of spontaneous decays (unless stated otherwise). The temperature was measured directly at the sample holder window by a silicon diode sensor connected to a digital controller providing stabilization accuracy of 0.1 K.

The mid-IR spectra (4000−400 cm^{-1} range) were recorded using a Thermo Nicolet 6700 Fourier transform infrared spectrometer, equipped with a deuterated triglycine sulfate (DTGS) detector and a KBr beam splitter, with 0.5 cm^{-1} resolution. To avoid interference from atmospheric H_2O and CO_2, a stream of dry air was continuously purged through the optical path of the spectrometer. In some experiments, to avoid exposing the sample matrix to the light source of the FTIR spectrometer with wavenumbers higher than 2200 cm^{-1}, the mid-IR spectra were recorded only in the 2200−400 cm^{-1} range, with a standard Edmund Optics long-pass filter placed between the spectrometer sources and the cryostat.

UV−vis Irradiation Experiments. The matrices were irradiated, through the outer KBr window of the cryostat, using tunable narrowband (~0.2 cm^{-1} spectral width) light provided by a signal

Scheme 3. Summary of the Reactions Experimentally Observed on the Potential Energy Surface of the Aryl Nitrene 2

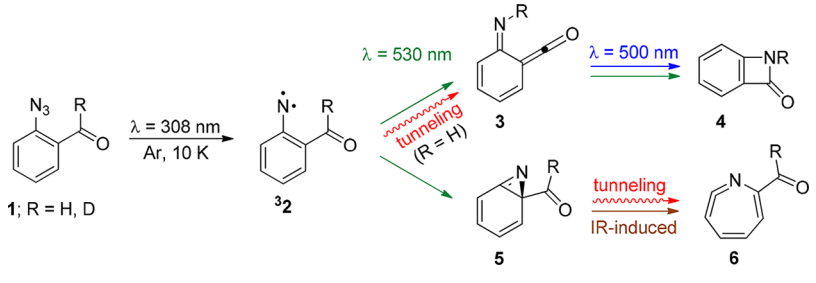

DOI: 10.1021/jacs.7b10495
J. Am. Chem. Soc. 2017, 139, 17649−17659

(visible light) or a frequency-doubled signal (UV range) beam of the Spectra Physics Quanta-Ray MOPO-SL optical parametric oscillator pumped with a pulsed Nd:YAG laser (repetition rate = 10 Hz, duration = 10 ns). The pulse energy for visible and UV-light irradiations was 9−10 and 1−3 mJ, respectively. Irradiation with UV light at 308 nm was used to induce the initial photochemistry of the azide precursor (**1**-h and **1**-d) because it matches its first absorption maximum and avoid, as much as possible, the absorption of corresponding product triplet nitrene (^{3}**2**-h and ^{3}**2**-d) with a maximum at around 326 nm.

Kinetics. Monitoring of the decays of **5**-d into **6**-d and of **5**-h into **6**-h was carried out by successive registrations of infrared spectra, as a function of time. For all of the three different sets of external light ("dark", "filtered IR light", and "unfiltered IR light", described above) the infrared spectra were collected using 64 scans. Under such conditions, the collection length of one spectrum equals to 261 s. Already during these initial minutes, a part of the photoproduced benzazirine **5** undergoes decay into cyclic ketenimine **6**. In the kinetic analysis, the moment of registration of the first spectrum was assumed to be the origin of decay time, the intensity of the benzazirine **5** bands present in this first spectrum was assumed to be relative 100%, and the amount of cyclic ketenimine **6** present extracted from the same first spectrum (formed between the irradiation and the registration of the first spectrum) was assumed to be relative 0%. The amounts of particular species in the sample were followed by the peak intensities of the most characteristic absorption bands, nonoverlapping with absorptions of other species. For this purpose, the following peaks were selected: 1241 cm^{-1} for **5**-d (Table 1), 1890 cm^{-1} for **6**-d (Table 2), 1242 cm^{-1} for **5**-h (Table S7), and 1883 cm^{-1} for **6**-h (Table S8). For "unfiltered IR light" kinetics (Figure 6), the decay of **5**-d was monitored for 32 h and, upon that time, ∼20% of the benzazirine remained in the sample. The "dark" decay kinetics of **5**-d (Figure 7, left) was monitored for 120 h and, upon that time, ∼ 75% of benzazirine **5**-d still remained in the sample. After that period, the "unfiltered IR light" conditions were implemented, and the decay was followed during subsequent 65 h (Figure 7, right). During that time, the amount of benzazirine **5**-d decreased from ∼75% to just ∼5%. In a similar experiment with the protium analogue **5**-h, ∼73% of benzazirine **5**-h remained in the sample after 120 h of applying "dark" conditions. After subsequent 72 h of observation using the "unfiltered IR light conditions", the amount of **5**-h decreased from ∼73% to less than 5%. The amounts of cyclic ketenimine **6** generated in the process of tunneling were then normalized in such a way so that at the end of each monitoring period the sum of **5** and **6** would be 100%. These normalizations assumed a direct quantitative transformation of **5** into **6**, which was indeed confirmed spectroscopically. The decays observed in present experiments (presented in Figures 6, 7, S8 and S9) were fitted, for rough estimation of the rate constants, using the equations of a single-exponential decay: $[R]_t = [R]_0 \exp[-kt]$. The rate constants k extracted from these fits, and the corresponding half-lives, are discussed in the text.

Theoretical Calculations. Calculations performed at the B3LYP/6-311++G(d,p) level were carried out using Gaussian09.[47] With the aim of modeling the IR spectra, geometry optimizations at the B3LYP/6-311++G(d,p) level were followed by harmonic frequency calculations at the same level. To correct the vibrational anharmonicity, basis set truncation, and the neglected part of electron correlation, the calculated frequencies were scaled by 0.98[48] (0.97 for the ν(N−D) mode). The scaled frequencies and the calculated IR intensities were then convoluted with Lorentzian functions having an fwhm = 2 cm^{-1}. The integral area of the simulated band equals to the theoretical calculated IR intensity. Due to the broadening, the peak intensities in the simulated spectra are reduced compared with the calculated intensities (in km mol^{-1}) and, therefore, are shown in arbitrary units of "relative intensity". Assignments of vibrational modes were made by inspection of ChemCraft[49] animations.

Tunneling Calculations. Single-point energy values were computed at the CCSD(T)-F12/cc-pVTZ-F12//M06-2X/6-311+G-(2d,p) level[50−52] (coupled cluster computations were carried out with ORCA[53] version 4.0.1, DFT optimizations with Gaussian09[47]). All of the computed reaction rates including quantum tunneling were carried out using a multidimensional small curvature tunneling method (SCT),[54] with step size of 0.001 Bohr, quantized reactant state tunneling (QRST) for the reaction coordinate mode, and at the M06-2X/6-311+G(2d,p) level. Using a multidimensional method to account for "corner-cutting" was critical, as the rate constants obtained using the unidimensional zero-curvature tunneling (ZCT) are 3 orders of magnitude less for this reaction. All the rates were computed with Polyrate,[55] using Gaussrate[56] as the interface with Gaussian.

■ ASSOCIATED CONTENT

Supporting Information

The Supporting Information is available free of charge on the ACS Publications website at DOI: 10.1021/jacs.7b10495.

Additional experimental results, IR assignments, and computational data (PDF)

■ AUTHOR INFORMATION

Corresponding Author

*E-mail: cmnunes@qui.uc.pt.

ORCID

Cláudio M. Nunes: 0000-0002-8511-1230
Igor Reva: 0000-0001-5983-7743
Sebastian Kozuch: 0000-0003-3070-8141
Robert J. McMahon: 0000-0003-1377-5107
Rui Fausto: 0000-0002-8264-6854

Notes

The authors declare no competing financial interest.

■ ACKNOWLEDGMENTS

This work was supported by the Portuguese "Fundação para a Ciência e a Tecnologia" (FCT). The Coimbra Chemistry Centre is supported by the FCT through the project UID/QUI/0313/2013, cofunded by COMPETE. C.M.N. and I.R. acknowledge the FCT for Postdoctoral Grant No. SFRH/BPD/86021/2012 and Investigador FCT Grant, respectively. S.K. acknowledges the support of the Israel Science Foundation (grant 631/15). R.J.M. acknowledges support from the U.S. National Science Foundation (CHE-1362264 and CHE-1664912).

■ REFERENCES

(1) *Nitrenes and Nitrenium Ions*; Falvey, D. E., Gudmundsdóttir, A. D., Eds.; John Wiley & Sons, 2013.
(2) Gritsan, N.; Platz, M. S. Photochemistry of Azides: The Azide/Nitrene Interface. In *Organic Azides: Syntheses and Applications*; Bräse, S., Banert, K., Eds.; John Wiley & Sons, 2010; pp 311−372.
(3) Platz, M. S. Nitrenes. In *Reactive Intermediate Chemistry*; Moss, R. A., Platz, M. S., Jones, M. J., Eds.; John Wiley & Sons, 2004; pp 501−559.
(4) Gritsan, N.; Borden, W. T.; Platz, M. The Study of Nitrenes by Theoretical Methods. In *Computational Methods in Photochemistry*; Kutateladze, A. G., Eds.; CRC Press, 2005; pp 235−356.
(5) Wentrup, C. *Chem. Rev.* **2017**, *117*, 4562−4623.
(6) Gritsan, N. P.; Platz, M. S. *Chem. Rev.* **2006**, *106*, 3844−3867.
(7) Borden, W. T.; Gritsan, N. P.; Hadad, C. M.; Karney, W. L.; Kemnitz, C. R.; Platz, M. S. *Acc. Chem. Res.* **2000**, *33*, 765−771.
(8) Smith, E.; Collins, I. *Future Med. Chem.* **2015**, *7*, 159−183.
(9) Tasdelen, M. A.; Yagci, Y. *Angew. Chem., Int. Ed.* **2013**, *52*, 5930−5938.
(10) Liu, L.; Yan, M. *Acc. Chem. Res.* **2010**, *43*, 1434−1443.
(11) Bräse, S.; Gil, C.; Knepper, K.; Zimmermann, V. *Angew. Chem., Int. Ed.* **2005**, *44*, 5188−5240.

DOI: 10.1021/jacs.7b10495
J. Am. Chem. Soc. 2017, 139, 17649−17659

(12) Lineberger, W. C.; Borden, W. T. *Phys. Chem. Chem. Phys.* **2011**, *13*, 11792−11813.
(13) Wijeratne, N. R.; Da Fonte, M.; Ronemus, A.; Wyss, P. J.; Tahmassebi, D.; Wenthold, P. G. *J. Phys. Chem. A* **2009**, *113*, 9467−9473.
(14) Karney, W.; Borden, W. *J. Am. Chem. Soc.* **1997**, *119*, 1378−1387.
(15) Inui, H.; Sawada, K.; Oishi, S.; Ushida, K.; McMahon, R. J. *J. Am. Chem. Soc.* **2013**, *135*, 10246−10249.
(16) Grote, D.; Sander, W. *J. Org. Chem.* **2009**, *74*, 7370−7382.
(17) Pritchina, E. A.; Gritsan, N. P.; Bally, T. *Phys. Chem. Chem. Phys.* **2006**, *8*, 719−727.
(18) Morawietz, J.; Sander, W. *J. Org. Chem.* **1996**, *61*, 4351−4354.
(19) Nunes, C. M.; Knezz, S. N.; Reva, I.; Fausto, R.; McMahon, R. J. *J. Am. Chem. Soc.* **2016**, *138*, 15287−15290.
(20) Gerbig, D.; Schreiner, P. R. *Angew. Chem., Int. Ed.* **2017**, *56*, 9445−9448.
(21) Ley, D.; Gerbig, D.; Schreiner, P. R. *Org. Biomol. Chem.* **2012**, *10*, 3781−3790.
(22) Layfield, J. P.; Hammes-Schiffer, S. *Chem. Rev.* **2014**, *114*, 3466−3494.
(23) Lambert, N.; Chen, Y.-N.; Cheng, Y.-C.; Li, C.-M.; Chen, G.-Y.; Nori, F. *Nat. Phys.* **2012**, *9*, 10−18.
(24) Borden, W. T. *WIREs Comput. Mol. Sci.* **2016**, *6*, 20−46.
(25) Two possible additional cases of heavy-atom tunneling are the ring-closure reactions of triplet 1,3-diradicals, cyclopentane-1,3-diyl, and cyclobutane-1,3-diyl. See refs 25a and 25b, respectively. Because both reactions require that the triplet 1,3-diradical undergoes ISC to form the singlet product, the rationalization of the mechanism involved is more complex. (a) Buchwalter, S. L.; Closs, G. L. *J. Am. Chem. Soc.* **1979**, *101*, 4688−4694. (b) Sponsler, M. B.; Jain, R.; Coms, F. D.; Dougherty, D. A. *J. Am. Chem. Soc.* **1989**, *111*, 2240−2252.
(26) Orendt, A. M.; Arnold, B. R.; Radziszewski, J. G.; Facelli, J. C.; Malsch, K. D.; Strub, H.; Grant, D. M.; Michl, J. *J. Am. Chem. Soc.* **1988**, *110*, 2648−2650.
(27) Zuev, P. S.; Sheridan, R. S.; Albu, T. V.; Truhlar, D. G.; Hrovat, D. A.; Borden, W. T. *Science* **2003**, *299*, 867−870.
(28) Moss, R. A.; Sauers, R. R.; Sheridan, R. S.; Tian, J.; Zuev, P. S. *J. Am. Chem. Soc.* **2004**, *126*, 10196−10197.
(29) Ertelt, M.; Hrovat, D. A.; Borden, W. T.; Sander, W. *Chem. - Eur. J.* **2014**, *20*, 4713−4720.
(30) Schleif, T.; Mierez-Perez, J.; Henkel, S.; Ertelt, M.; Borden, W. T.; Sander, W. *Angew. Chem., Int. Ed.* **2017**, *56*, 10746−10749.
(31) Nandi, A.; Gerbig, D.; Schreiner, P. R.; Borden, W. T.; Kozuch, S. *J. Am. Chem. Soc.* **2017**, *139*, 9097−9099.
(32) Only the *anti*-form of the deuterated 2-formylphenylazide **1**-d precursor, considering the orientation of the −CDO moiety, was populated in the gas phase and deposited in the matrix. Accordingly, only the *anti*-form of nitrene ^{3}**2**-d was generated in the matrix upon photolysis of **1**-d (see also ref 19).
(33) In the experimental difference UV−vis spectrum obtained for triplet nitrene ^{3}**2** (ref 19), the presence of a strong absorption above 350 nm due to iminoketene **3** precluded the identification of weaker absorptions due to the nitrene in this region. However, the occurrence of photochemistry for ^{3}**2** with onset at 530 nm is coherent with the estimation of very weak electronic transitions at 449 and 536 nm by TDDFT calculations (ref 19). Indeed, it has been observed experimentally that triplet arylnitrenes have a characteristic weak feature that extends to 500 nm or higher; see ref 6 and: (a) Carra, C.; Nussbaum, R.; Bally, T. *ChemPhysChem* **2006**, *7*, 1268−1275.
(34) The conversion of **A** into **B** was also observed during irradiations at 530 nm, but the reaction is much more efficient at 500 nm.
(35) Nunes, C. M.; Reva, I.; Pinho e Melo, T. M. V. D.; Fausto, R. *J. Org. Chem.* **2012**, *77*, 8723−8732.
(36) Dunkin, I. R.; Lynch, M. A.; Withnall, R.; Boulton, A. J.; Henderson, N. *J. Chem. Soc., Chem. Commun.* **1989**, 1777.
(37) Breda, S.; Lapinski, L.; Reva, I.; Fausto, R. *J. Photochem. Photobiol., A* **2004**, *162*, 139−151.
(38) Tomioka, H.; Ichikawa, N.; Komatsu, K. *J. Am. Chem. Soc.* **1993**, *115*, 8621−8626.
(39) Chapman, O. L.; Le Roux, J. P. *J. Am. Chem. Soc.* **1978**, *100*, 282.
(40) Dunkin, I. R.; Thomson, P. C. P. *J. Chem. Soc., Chem. Commun.* **1980**, 499−501.
(41) Donnelly, T.; Dunkin, I. R.; Norwood, D. S. D.; Prentice, A.; Shields, C. J.; Thomson, P. C. P. *J. Chem. Soc., Perkin Trans. 2* **1985**, 307−310.
(42) Bally et al. have developed a protocol of irradiations allowing the selective photoconversion between the three isomeric species in cryogenic matrices: 2,6-difluorophenylnitrene, the corresponding benzazirine, and cyclic ketenimine. The approach was based on their different UV−vis absorption spectra (see ref 33a): triplet arylnitrenes have a characteristic weak feature that extends to 500 nm or more, benzazirines have a broad feature around 300 nm, and the corresponding cyclic ketenimines have a broad band around 400 nm. A similar protocol was applied by other authors (see refs 15, 16, 42a, and 42b). In the present case, the study of photochemical interconversions between triplet arylnitrene ^{3}**2**, benzazirine **5**, and cyclic ketenimine **6** might be hampered by an additional photochemical pathway from nitrene ^{3}**2** to iminoketene **3** (which is also photoreactive) and the existence of two tunneling reactions. (a) Sander, W.; Winkler, M.; Cakir, B.; Grote, D.; Bettinger, H. F. *J. Org. Chem.* **2007**, *72*, 715−724. (b) Grote, D.; Finke, C.; Neuhaus, P.; Sander, W. *Eur. J. Org. Chem.* **2012**, *2012*, 3229−3236.
(43) The IR light source (ETC EverGlo) of our FTIR spectrometer, running in normal operating mode, produces radiation essentially only in the 7400 to 50 cm^{-1} region. This clearly rules out the possibility of the rearrangement of **5** to **6** being promoted by an electronic transition, when the sample is kept under "unfiltered IR light" conditions. Actually, if any radiation capable of inducing electronic excitation reached the sample under "unfiltered IR light" conditions, one would expect the observation of **3** to **4** rearrangement. As described, the rearrangement of **3** to **4** is induced by irradiation at 500 nm, and at this wavelength species **5** does not absorb (TDDFT calculation estimates the first electronic transition of **5** at λ = 332 nm [f = 0.0093]).
(44) Examples of isomerization reactions in matrices that consist of two components, tunneling and IR-induced conversion (which may compete), have been previously described. See ref 30 and: (a) Reva, I.; Nunes, C. M.; Biczysko, M.; Fausto, R. *J. Phys. Chem. A* **2015**, *119*, 2614−2627. (b) Lapinski, L.; Reva, I.; Rostkowska, H.; Fausto, R.; Nowak, M. J. *J. Phys. Chem. B* **2014**, *118*, 2831−2841. (c) Reva, I.; Nowak, M. J.; Lapinski, L.; Fausto, R. *J. Chem. Phys.* **2012**, *136*, 64511.
(45) Some of us have been working on the predictions of heavy-atom tunneling using SCT computations. For some of the most recent works, see: (a) Kozuch, S. *Phys. Chem. Chem. Phys.* **2014**, *16*, 7718−7727. (b) Kozuch, S.; Zhang, X.; Hrovat, D. A.; Borden, W. T. *J. Am. Chem. Soc.* **2013**, *135*, 17274−17277.
(46) Zhang, X.; Datta, A.; Hrovat, D. A.; Borden, W. T. *J. Am. Chem. Soc.* **2009**, *131*, 16002−16003.
(47) Frisch, M. J.; Trucks, G. W.; Schlegel, H. B.; Scuseria, G. E.; Robb, M. A.; Cheeseman, J. R.; Scalmani, G.; Barone, V.; Mennucci, B.; Petersson, G. A.; Nakatsuji, H.; Caricato, M.; Li, X.; Hratchian, H. P.; Izmaylov, A. F.; Bloino, J.; Zheng, G.; Sonnenberg, J. L.; Hada, M.; Ehara, M.; Toyota, K.; Fukuda, R.; Hasegawa, J.; Ishida, M.; Nakajima, T.; Honda, Y.; Kitao, O.; Nakai, H.; Vreven, T.; Montgomery, J. A., Jr.; Peralta, J. E.; Ogliaro, F.; Bearpark, M.; Heyd, J. J.; Brothers, E.; Kudin, K. N.; Staroverov, V. N.; Keith, T.; Kobayashi, R.; Normand, J.; Raghavachari, K.; Rendell, A.; Burant, J. C.; Iyengar, S. S.; Tomasi, J.; Cossi, M.; Rega, N.; Millam, J. M.; Klene, M.; Knox, J. E.; Cross, J. B.; Bakken, V.; Adamo, C.; Jaramillo, J.; Gomperts, R.; Stratmann, R. E.; Yazyev, O.; Austin, A. J.; Cammi, R.; Pomelli, C.; Ochterski, J. W.; Martin, R. L.; Morokuma, K.; Zakrzewski, V. G.; Voth, G. A.; Salvador, P.; Dannenberg, J. J.; Dapprich, S.; Daniels, A. D.; Farkas, Ö.; Foresman, J. B.; Ortiz, J. V.; Cioslowski, J.; Fox, D. J. *Gaussian 09*, revision D.01; Gaussian, Inc.: Wallingford, CT, 2013.
(48) Nunes, C. M.; Reva, I.; Fausto, R.; Begue, D.; Wentrup, C. *Chem. Commun.* **2015**, *51*, 14712−14715.

DOI: 10.1021/jacs.7b10495
J. Am. Chem. Soc. 2017, 139, 17649−17659

(49) Zhurko, G. A. *ChemCraft, Version 1.8*. http://www.chemcraftprog.com, 2016 (last accessed on Nov 3, 2017).
(50) Ten-no, S.; Noga, J. *WIREs Comput. Mol. Sci.* **2012**, *2*, 114−125.
(51) Zhao, Y.; Truhlar, D. G. *Theor. Chem. Acc.* **2008**, *120*, 215−241.
(52) Peterson, K. A.; Adler, T. B.; Werner, H. J. *J. Chem. Phys.* **2008**, *128*, 84102.
(53) Neese, F. *WIREs Comput. Mol. Sci.* **2012**, *2*, 73−78.
(54) Fernandez-Ramos, A.; Ellingson, B. A.; Garrett, B. C.; Truhlar, D. G. In *Reviews in Computational Chemistry*; Lipkowitz, K. B., Cundari, T. R., Eds.; John Wiley & Sons, 2007; Vol. 3, pp 125−232.
(55) Zheng, J.; Bao, J. L.; Meana-Pañeda, R.; Zhang, S.; Lynch, B. J.; Corchado, J. C.; Chuang, Y.-Y.; Fast, P. L.; Hu, W.-P.; Liu, Y.-P.; Lynch, G. C.; Nguyen, K. A.; Jackels, C. F.; Fernandez Ramos, A.; Ellingson, B. A.; Melissas, V. S.; Villà, J.; Rossi, I.; Coitiño, E. L.; Pu, J.; Albu, T. V.; Ratkiewicz, A.; Steckler, R.; Garrett, B. C.; Isaacson, A. D.; Truhlar, D. G. *Polyrate*, version 2016-2A; University of Minnesota, Minneapolis, 2016.
(56) Zheng, J.; Zhang, S.; Corchado, J. C.; Meana-Pañeda; Chuang, Y.-Y.; Coitiño, E. L.; Ellingson, B. A.; Truhlar, D. G.; *Gaussrate*; Department of Chemistry and Supercomputing Institute, University of Minnesota, Minneapolis, MN, 2016; p 55455.

NOTE ADDED IN PROOF

Recently, a paper reporting fast heavy-atom tunneling in trifluoroacetyl nitrene was published by Z. Wu, R. Feng, H. Li, J. Xu, G. Deng, M. Abe, D. Begue, K. Liu, and X. Zeng. See *Angew. Chem., Int. Ed.* **2017**, DOI: 10.1002/anie.201710307. Heavy-atom tunneling in the C−H insertion of a singlet carbene was reported by P. Zuev and R. S. Sheridan. See *J. Am. Chem. Soc.* **1994**, *116*, 4123−4124.

DOI: 10.1021/jacs.7b10495
J. Am. Chem. Soc. 2017, 139, 17649−17659